nzsee
NEW ZEALAND SOCIETY FOR EARTHQUAKE ENGINEERING

Damage Level Prediction of RC Building for Future Earthquakes Based on Seismic Response Observation

Z.Yi, A. Oono, J.Monical, & M. Maeda
Tohoku University, Sendai, Japan.

M. Seki
Building Research Institute, Tokyo, Japan.

ABSTRACT

Estimating the performance curve and evaluating the damage level in structures for both past and future possible earthquakes is essential but challenging. This paper proposes a characteristic point method for the updating of the performance curve and damping based on the observed seismic response and analytical model, further predicting the response and evaluating the damage level corresponding to the future possible earthquake.

A single-degree-of-freedom system is proposed to verify the influence of the accuracy of analyzation on the accuracy of the methods. First, by considering the output of the time-history analysis as the observation, a trial calculation is carried out to verify the performance of the proposed methods compared with the condition without applying the method. Then, a series of cases are considered to investigate the applicability of the proposed methods by 1) limiting the observed range to a maximum ductility factor of 1.2, and 2) introducing artificial error in the analytical model by modifying initial stiffness, yielding stiffness, using factors between -40% to 40%, and cracking strength, yielding strength using factors between -20% to 20%.

The proposed methods were observed to increase the accuracy of the prediction of response and damage level corresponding to future earthquakes. With the increase of the accuracy of the analytical model, the prediction of the characteristic points and future response becomes much more accurate, leading to a better prediction of the damage level corresponding to the future possible earthquake.

1 INTRODUCTION

Reinforced concrete structures should be evaluated for damage quickly after intense earthquakes (Datta et al. 2010). By surveying damaged structures, engineers can judge the current condition of the structure and predict damage in future ground motions. However, quantifying damage through visual inspection requires time and skilled labour. A structural health monitoring (SHM) system is a viable alternative solution because it can record drift and acceleration demands of the structure and output observations automatically (Xu et al. 2021). By setting the relationship between the observation from SHM system and the damage level, the damage condition of a structure can be determined (Miura et al. 2021). Besides, if the response of the structure corresponding to the future possible earthquake can be predicted, the safety of a structure in future earthquake motions can be evaluated.

In practical utilization, the safety of a structure in future earthquake motions can be evaluated using seismic demand and structural performance curves in the method known as the Capacity Spectrum Method (CSM) (Yi et al. 2023). Until now, the method for predicting the response and damage level has been developed, but the accuracy of prediction is not fully studied. It is obvious that the accuracy of the future prediction relies on the accuracy of the updated performance curve and damping. Nevertheless, the quantitative relationship between the updated performance and the accuracy of the prediction is not clear.

The purpose of this paper is to evaluate the accuracy of the updating method in estimating seismic response and damage level over a range of input parameters. Changes in parameters including stiffness, strength, and damping, produce variation between observed and updated performance and damping curves which are used as indices to judge the accuracy of the method. The research goals are to 1) evaluate quantitatively the effectiveness of the proposed updating method when applied to a range of cases where the analytical model and observed behaviour differ, and 2) summarize qualitatively the influence of changes in initial setting on accuracy of prediction.

2 OUTLINE OF REASEARCH

2.1 Methodology for predicting response and damage level

The basic concepts for updating performance and damping curves and predicting future response and damage level are described in this section. In this study, a single-degree-of-freedom (SDOF) system is considered for the analytical model. As shown in Fig1(a), using the output of the analytical model and observed data, two performance curves are estimated: the analytical performance curve, which comes from the pushover analysis of the analytical model; and the observed performance curve, which is estimated from the acceleration-displacement records.

The observed damping factors are evaluated using the Capacity Spectrum Method, as illustrated in Fig1(b). The method estimates seismic demand as the intersection of the response spectrum and performance curve. To estimate a plausible damping factor h associated with the observed response, damping is incrementally increased to reduce the response spectrum in an iterative fashion until the intersection of the curves produces a solution equivalent to the measured response.

After that, the Takeda model defines cracking and yielding in load-displacement relationships for reinforced concrete structures is studied here to describe the relationship between ductility factor and analytical damping before and after yielding (Fig. 15). Analytical damping is computed as the ratio of energy dissipation (blue area) to maximum elastic potential energy (yellow area).

In Fig.1(c), the schematic flow diagram of the described procedure is shown with the following four steps. 1) the analytical performance curve is updated to match peak response observed in past earthquakes, 2) the analytical damping model is updated based on observed damping factors inferred from results of CSM, 3) the

damage level is classified based on regions defined using the updated performance curve, and 4) the expected response and damage level is predicted using CSM, updated performance curve, and updated damping curve. The detailed procedures are discussed as follows.

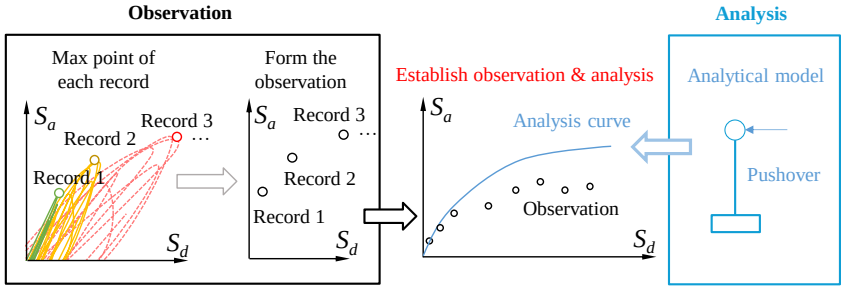

(a) establish observation and analyzation (performance curve)

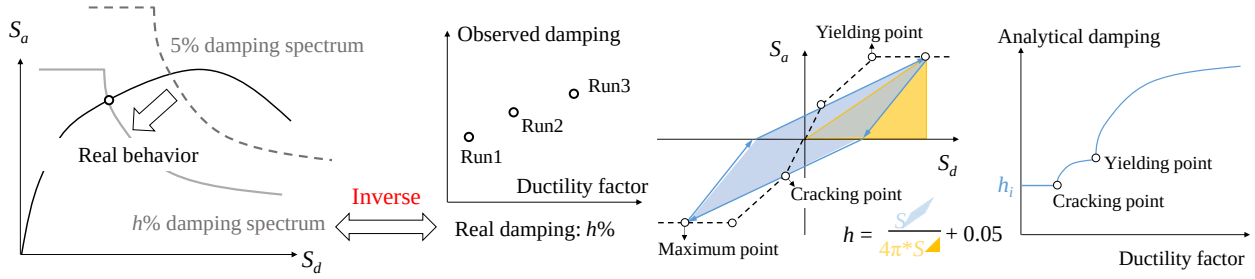

(b) establish observation and analyzation (damping)

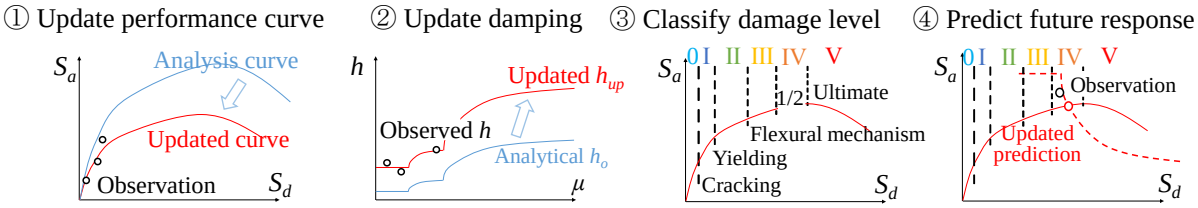

(c) prediction for the future response

Figure 1: General flow of evaluation

2.1.1 Updating performance curve

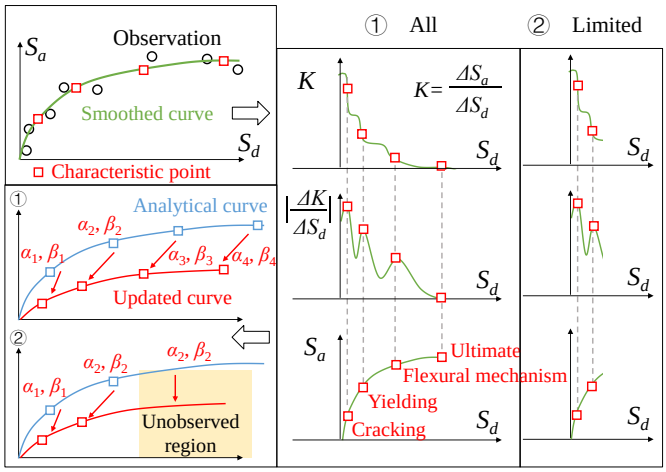

Figure 2: Updating of performance curve

The updating of performance curve is illustrated in Fig. 3. First, a smooth curve is fitted to observed points using Kalman filtering. Then, the tangent stiffness and rate of change of tangent stiffness are calculated. Several observed characteristic points are identified using peak values of the rate of change of stiffness. Analytical characteristic points are obtained using the same procedure as that used for observed characteristics points. Finally, the updated performance curve is generated by fitting each analytical point to the appropriate observed characteristic point using a set of amplification factors α_i and β_i for S_a and S_d. In the case where only one or two characteristic points are available because of a limited range of observation, the

amplification factors corresponding to the characteristic point furthest from the origin are utilized to update the performance curve in the unobserved region.

2.1.2 Updating damping curve

The updating of the damping curve is clarified, as shown in Fig 3. Two conditions are considered based on the number of characteristic points identified in Sec. 2.1.1.

1). Have all characteristic points. By fitting the observed and analytical damping factor with several amplification factors in each region between two continuous characteristic points, the analytical damping factor is updated.

2). Have limited characteristic points (e.g., only cracking). Before cracking, the updated damping factor is constant and is equal to the average observed damping factor. After cracking and before yielding, an amplification factor a_2 is calculated to fit the analytical damping with the observed damping. Damping is predicted in the unobserved region by updating the analytical damping using the same amplification factor.

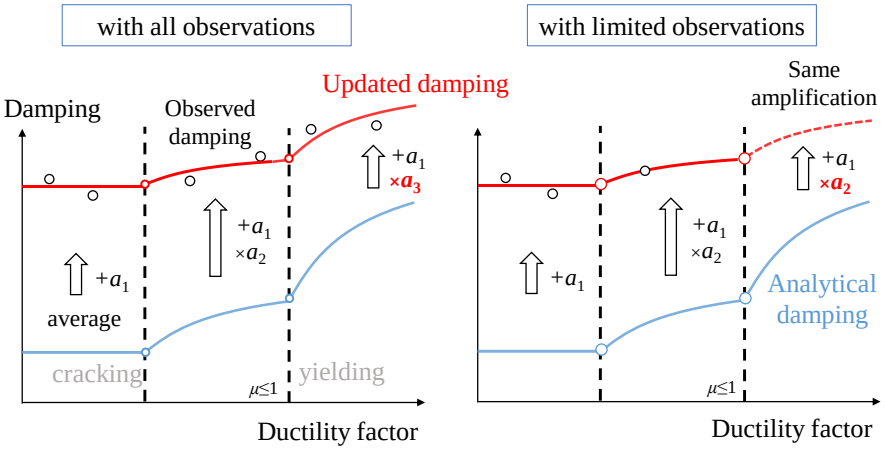

Figure 3: Updating of damping curve

2.1.3 Identifying damage level

According to previous research (Miura et al. 2021, Yi et al.2023), the damage level can be roughly defined using structural response. The characteristic points identified in Sec. 2.1.1 are related to the damaged behaviour of the structure. Hence, S_d of characteristic points is assumed to represent a reasonable boundary between distinct levels of damage. The relationship between the selected characteristic points and damage levels is shown in Fig.4. The boundary between damage levels III and IV is not clear. Hence, the midpoint between the S_d at the flexural mechanism and ultimate state points is set to represent the boundary between moderate and severe damage.

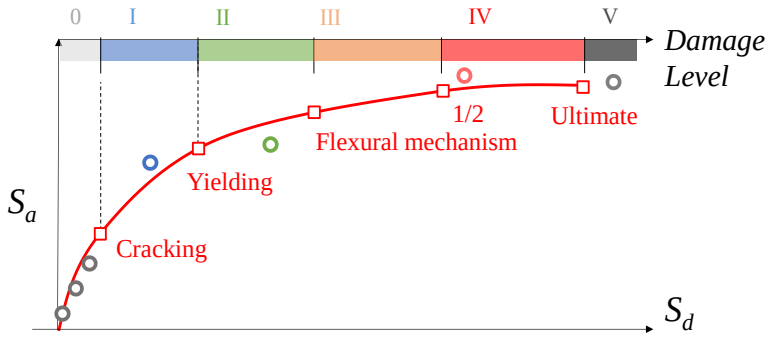

Figure 4: Damage level classification

2.1.4 Predicting future response and damage level

The future response is estimated using the CSM, as shown in Fig. 5. There are two kinds of prediction corresponding to the conditions with or without updating. Damage level is also predicted in the meantime based on the classification in Sec. 2.1.3.

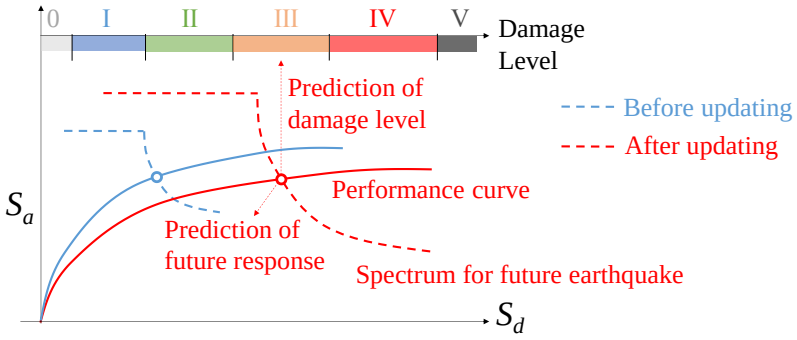

Figure 5: Prediction of future response and damage level

2.2 Evaluation of updated performance

The estimation of the error between the updated performance curve and the observed response is described in Fig. 6.

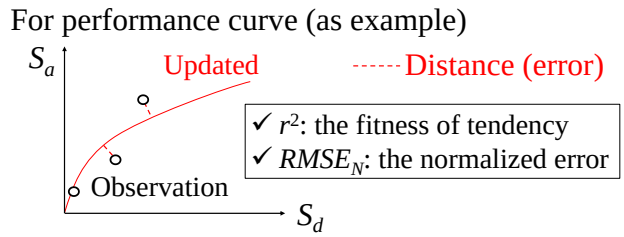

Figure 6: Accuracy of updated performance

Both the correlation efficiency (r^2) and normalized root mean square error ($RMSE_N$) defined by Eqs.1-2 are utilized to evaluate the accuracy of the updating method on the performance and damping curves.

$$r^2 = \frac{Cov(obs,ana)}{\sqrt{Var(obs)\times Var(ana)}} \quad (1)$$

where obs = data vectors of the observed analytical performance or damping curve; ana = data vectors of the updated analytical performance or damping curve.

$$RMSE_N = \frac{1}{obs_{max}}\sqrt{\frac{\sum(obs_i - ana_i)^2}{n}} \quad (2)$$

where n = total number of the observed points; obs_{max} = maximum value among the observation vectors.

2.3 Evaluation of accuracy of future prediction

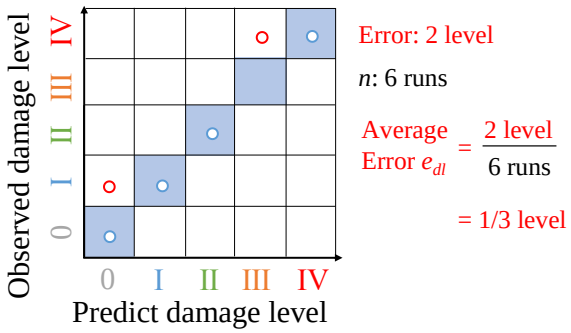

Figure 7: Accuracy of damage level

Considering the future response evaluated using spectral acceleration (S_a) and spectral displacement (S_d), the error in response err_r among all n points is evaluated by Eq. 3.

$$err_r = \frac{1}{n}\sum\frac{1}{2}\sqrt{\left(\frac{S_{ai-p}-S_{ai-o}}{S_{ai-o}}\right)^2 + \left(\frac{S_{di-p}-S_{di-o}}{S_{di-o}}\right)^2} \quad (3)$$

where S_{ai-p} and S_{ai-o} = predicted and observed S_a at point i; S_{di-p} and S_{di-o} = predicted and observed S_d at point i;

Regarding the accuracy in estimating damage level (example shown in Fig. 7), an absolute error e_{dl} is evaluated by comparing the observed and predicted

damage level $dlobs_i$ and $dlpre_i$ as defined by Eq. 4. To normalize this error and express it in relative terms (%), the error is divided by the maximum observed damage level $dlobs_{max}$ as defined in Eq. 5.

$$e_{dl} = \frac{\sum_1^n |dlobs_i - dlpre_i|}{n} \tag{4}$$

$$e_{dl-n} = \frac{e_{dl}}{dlobs_{max}} \tag{5}$$

3 SETTING OF ANALYTICAL MODEL

Based on the method proposed in previous work (Yi et al. 2023), the response and damage level are evaluated for a prototype structure. To verify the feasibility of the updating method on this structure, the methodology for evaluating accuracy is proposed and clarified next.

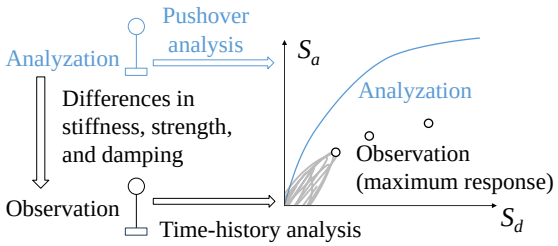

Figure 8: Concept of updating performance curve

To eliminate the influence of the error caused by higher modes, an equivalent single-degree-of-freedom (SDOF) system is utilized as the fundamental model. As shown in Fig. 8, the peak response of a nonlinear time-history analysis is taken as the observed result. The analytical performance curve is obtained from incremental pushover analysis. To evaluate realistic conditions where analysis and observation are likely to diverge from one another, artificial errors are introduced to produce differences between observation and analysis, and detailed settings are clarified as follows.

3.1 Analytical model

As Fig 9 shows, the Takeda model proposed by Takeda (1970) is utilized as the constitutive analysis model. Based on properties of a typical low-rise structure, the period is set to be 0.5s, the yielding stiffness is 30% of the initial stiffness, and the ultimate displacement is five times the yielding displacement. A summary of the parameters of the model are shown in Table 1.

Table 1: Basic properties of analytical model

Property	d_c	d_y	d_u	p_c	p_y	k_c	α	β	t	m
value	5.6	49.3	246.9	90	300	0.16	0.3	0.02	0.5	1000

(d_c, d_y, d_u: mm; p_c, p_y: gal; m: kg; k_c, k_y, ks_u: kN/mm; t: s)

where d_c and d_y = the cracking and yielding displacement, p_c and p_y = the cracking and yielding force, k_c = the initial stiffness. m is the mass. k_y and k_u = the yielding stiffness, and the stiffness after yielding, with α and β as the reduction factors.

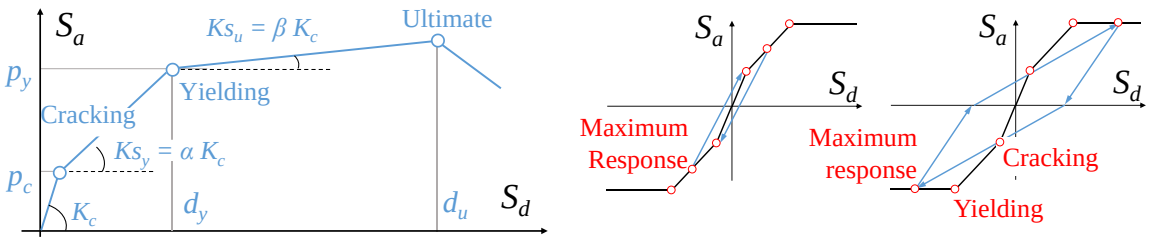

(a) Backbone curve (b) Hysteresis loop (before and after yielding)

Figure 9: Constitutive model of the analytical model

3.2 Observed model

In real conditions, the analytical model will inevitably differ from the observed behaviour of the structure. Hence, additional errors are introduced to both performance and damping curves of the observed model as shown in Fig.10. Errors introduced to each curve are explained next.

1). Performance curve: A set of errors, *m* and *n*, are utilized to adjust the values of the stiffness and lateral resistance associated with each region (cracking, yield, and ultimate points). As the error related to stiffness is typically much larger than the error related to strength based on structural design experience, the error in stiffness varies from -40% to +40%, and the error in strength varies from -20% to +20%.

2) Damping curve: The error in damping is introduced using different hysteretic models. In addition to the standard Takeda model, the Takeda slip model developed by Edo et al. (1977) is also considered which is expected to have smaller equivalent damping after yielding because of a reduction in the capacity for energy dissipation.

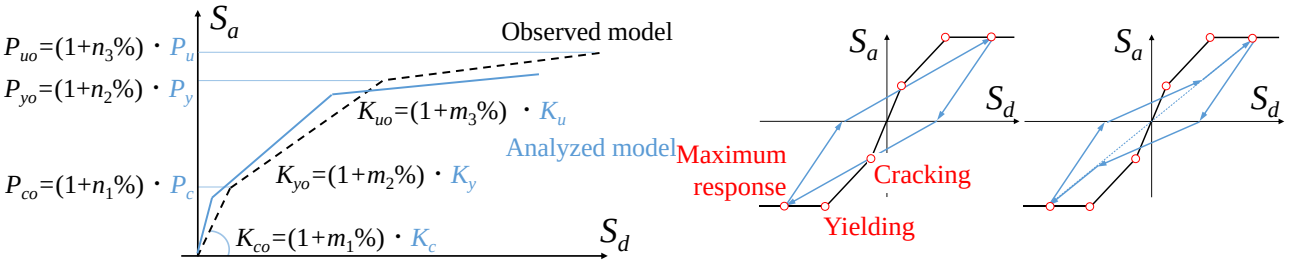

(a) Basic parameters (b) Loop setting (Takeda & Takeda slip model)

Figure 10: Constitutive model of the observation model

3.3 Damage evaluation method

The damage level is evaluated based on the relationship between the predicted response and the identified characteristic points, as shown in Fig.4. Because the Takeda model does not define the displacement at which the flexural mechanism or ultimate points are reached, a ductility factor, defined as the ratio of peak displacement to yield displacement, is used instead. Based on previous research (Yi et al. 2023), the response at ductility factors of 2 and 5 correspond approximately to the flexural mechanism and ultimate points.

3.4 Input ground motion

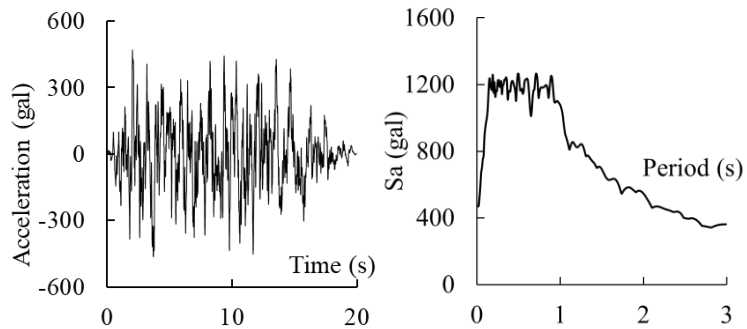

(a) time domain (b) frequency domain

Figure 11: Input ground motion

An artificial wave based on the 5% damped acceleration response spectra defined in the specifications of the Japanese Building Standard Law (JBSL) (2016) shown in Fig. 11 is selected as the input ground motion. Intensities of the observed runs are defined as shown in Table 2.

The earthquake intensity of a given run varies depending on the properties of the observed model. Nevertheless, for the same run, the response of each model produces the same ductility factor as defined in Eq. 6. In this paper, the maximum ductility factor of the observed response does not exceed 1.5. The ductility factors associated with predicting future response are set as 3 and 5 representing high-intensity earthquakes.

$$\mu = \frac{d}{d_y} \tag{6}$$

where μ = ductility factor, d = peak displacement corresponding to ductility factor μ, and d_y = yielding displacement.

Table 2: Setting of run intensities

Definition	Observation											Prediction	
Run	1	2	3	4	5	6	7	8	9	10	11	12	13
Expected μ	0.05	0.10	0.15	0.2	0.3	0.5	0.7	0.9	1.1	1.3	1.5	3	5

4 APPLICATION EXAMPLE OF PROPOSED METHOD

An example highlighting two cases with different amounts of error is described next to show the relationship between the updated performance and the accuracy of future response. Details of the cases are shown in Table 3. Predictions are made for runs producing ductility factors of 5.

Table 3: Setting of error parameters

Case	Stiffness			Strength			Damping*
	n_1	n_2	n_3	m_1	m_2	m_3	
1	0	0	0	0	0	0	a
2	-20	+20	+20	+20	-20	-20	b

*: a=Takeda model; b=Takeda slip model

4.1 Updating of performance curve

The updated performance curves for cases 1 and 2 are compared in Fig. 12, and the accuracy of the updated performance curve is listed in Table 4. Both cases produce an updated performance curve which matches well with observed response. Nevertheless, case 2 produces more error as a large initial difference is introduced to the performance curve.

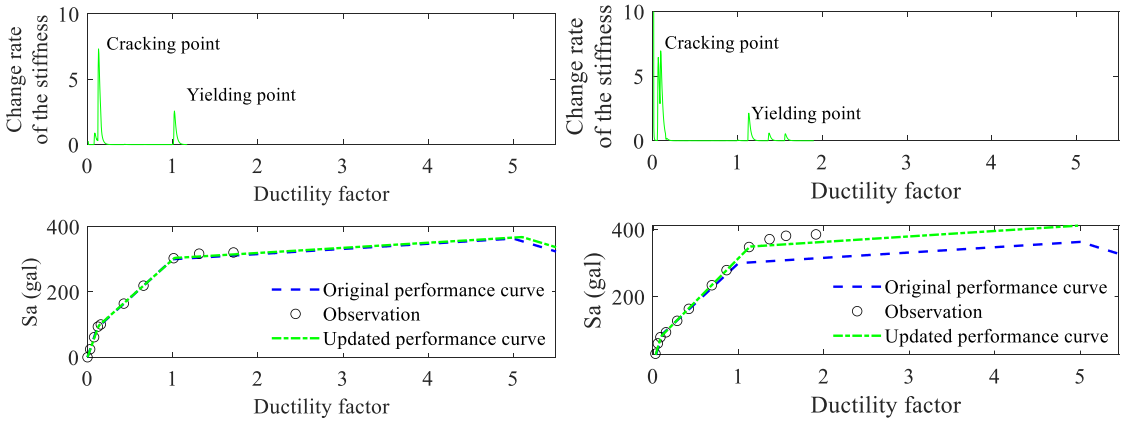

(a) Case 1 (b) Case 2

Figure 12: Updating of performance curve

Table 4: Accuracy of updated performance curve

Performance of performance curve		Value
Case 1	R^2	0.9997
	Normalized error (%)	1.12
Case 2	R^2	0.9881
	Normalized error (%)	3.09

4.2 Updating of damping

The updated damping for cases 1 and 2 is shown in Fig. 13 and Table 5. Both updated damping curves fit better with the observed damping compared with the original analytical damping model. The updated damping of case 1 shows a better fit as no error was introduced to original performance curve.

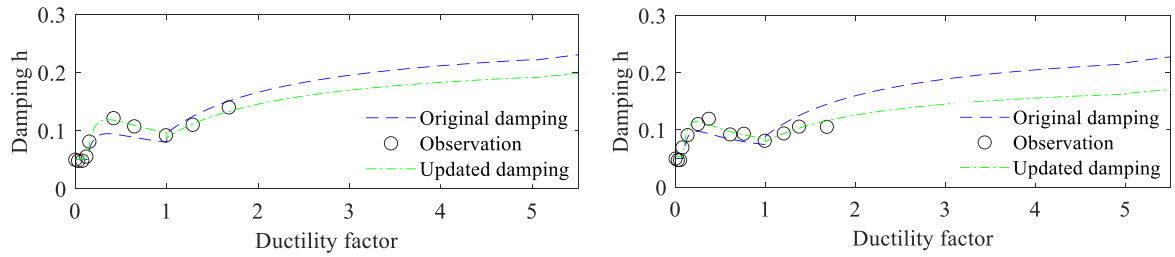

(a) Case 1 (b) Case 2

Figure 13: Updating of damping

Table 5: Accuracy of updated damping curve

Performance of performance curve		Value
Case 1	R^2	0.9859
	Normalized error (%)	2.47
Case 2	R^2	0.9472
	Normalized error (%)	5.92

4.3 Future response prediction

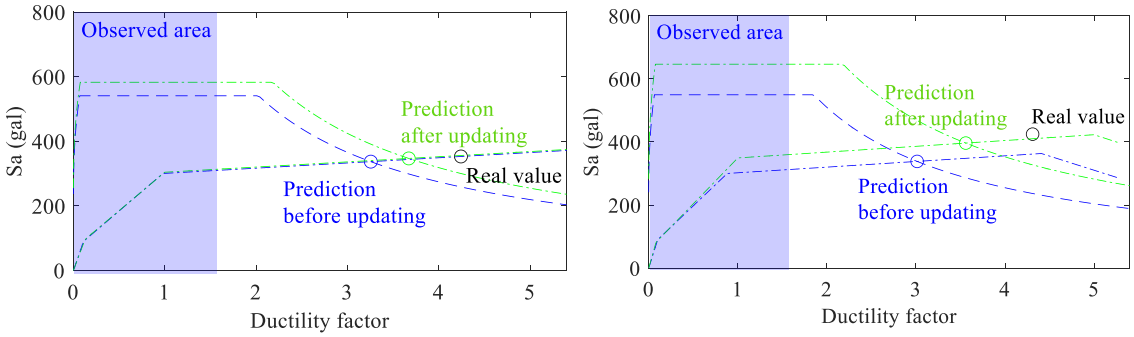

(a) Case 1 (b) Case 2

Figure 14: Future prediction

Based on the original and updated performance and damping curves, two predictions are estimated as illustrated in Fig. 14. After updating, the error of response prediction decreases from 17% to 9% for case 1, and from 26% to 13% for case 2, which indicates the proposed method produces a better prediction for the response in future earthquakes.

4.4 Relationship between updated performance and accuracy of response prediction

The results of the updated performance and prediction for cases 1 and 2 are shown in Fig. 15. Because the initial error introduced to case 2 is larger than that of case 1, the accuracy of the updated performance is worse for case 2. Also, the error in the prediction increases from 9% for case 1 to 13% for case 2, indicating that trends in error associated with updated performance can be used to described trends in future response prediction.

In Sec. 5, the results of 40 cases are presented and trends between accuracy of updated performance, predicted response, and damage level are described.

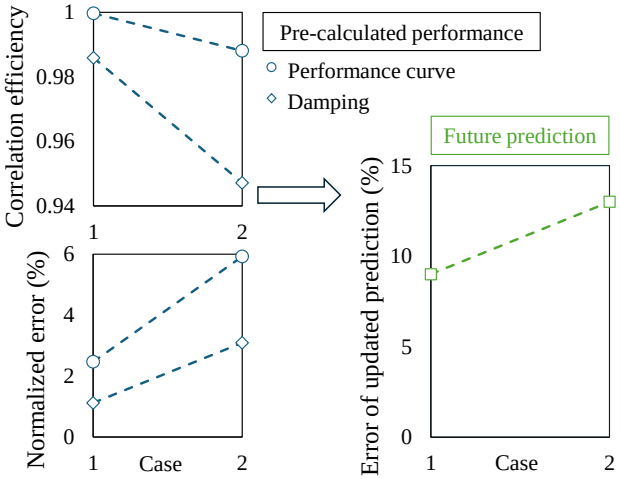

Figure 15: Updated performance & Accuracy of prediction

5 CASE STUDIES FOR PROPOSED METHOD

A set of cases is proposed considering plausible differences between analytical model and observed response. The accuracy of prediction and the applicable range of the proposed method is discussed.

5.1 Case setting

The analytical model is kept constant while the observed cases differ based on the errors listed in Table 7.

Table 7: Setting of the error parameters

Case	Stiffness			Strength			Damping*
	n_1	n_2	n_3	m_1	m_2	m_3	
1-8	±40	0	0	±20	0	0	a, b
9-16	0	±40	0	0	±20	0	a, b
17-24	0	0	±40	0	0	±20	a, b
25-40	±40	±40	0	±20	±20	0	a

*: a=Takeda model; b=Takeda slip model

In this way, the same original analytical model is adjusted to match different observed responses. The first set of cases (1-24) contain errors in cracking, yielding, and ultimate points. The second set of cases (25-40) contain errors in cracking and yielding points. A range of observations are considered with a maximum ductility factor of 1.5. Response associated with ductility factors of 3 and 5 are used to evaluate accuracy of the prediction.

5.2 Prediction of the cases

The error of the response prediction for each case with and without updating is shown in Fig. 16. Compared with response prediction before updating, approximately 80% of cases show a smaller error after updating, and the average error decreases from 20% to 11%. Hence, the proposed method can decrease error in prediction.

Then, the prediction of runs associated with ductility factors of 3 and 5 are compared in Fig. 17. As the ductility factor of the predicted run increases from 3 to 5, over 90% of the cases show a larger error, and the average error for all cases increases from 7% to 15%, which indicates the error of the proposed method tends to increase when the future response is larger. Nevertheless, the method seems to be effective for high-intensity earthquakes as average error does not exceed 15%.

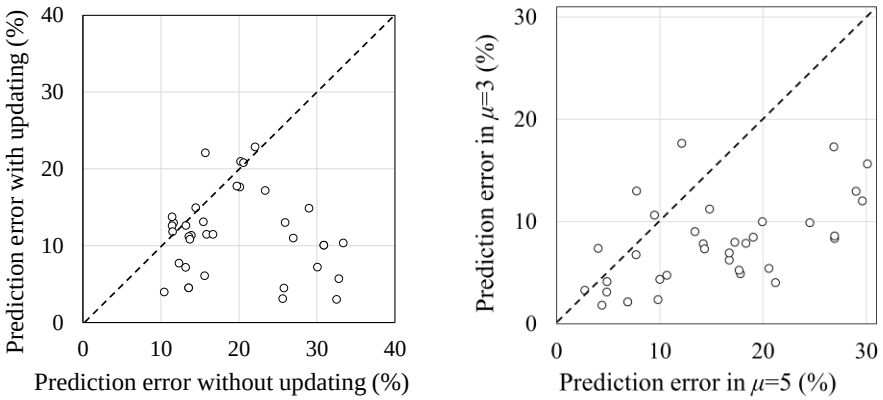

(a) with and without updating (b) with μ=3 and μ=5

Figure 16: Prediction of each cases

5.3 Updated performance & accuracy of prediction

The relationship between the updated performance and the accuracy of prediction is evaluated in this section. Response predictions of runs with ductility factors of 3 and 5 are investigated and the error is computed as the average error of both runs.

5.3.1 Performance curve

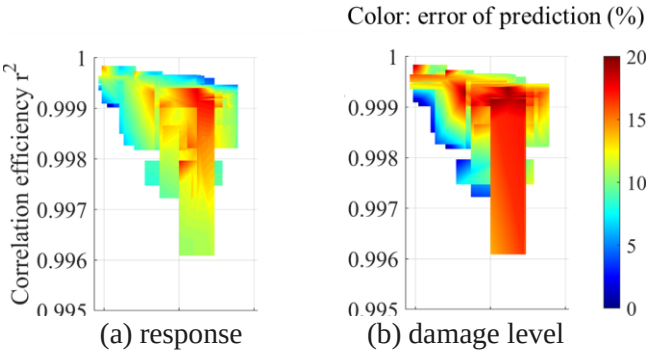

(a) response (b) damage level

Figure 17: Updated performance curve & prediction

Based on the error calculation described in Sec. 2, the relationship between the updated performance curve and the error of prediction is plotted in Fig. 17. The normalized error $RMSE_N$ and correlation efficiency r^2 are plotted as the x and y-coordinates, and the color in the figure represents the degree of the prediction error.

A minimum r^2 of 0.995 and a maximum $RMSE_N$ of 16% indicate the feasibility of the proposed method for updating the performance curve. However, for

both the predicted response and damage level evaluation, the accuracy of updated performance curve seems to have a weak influence on the accuracy of prediction.

5.3.2 Damping

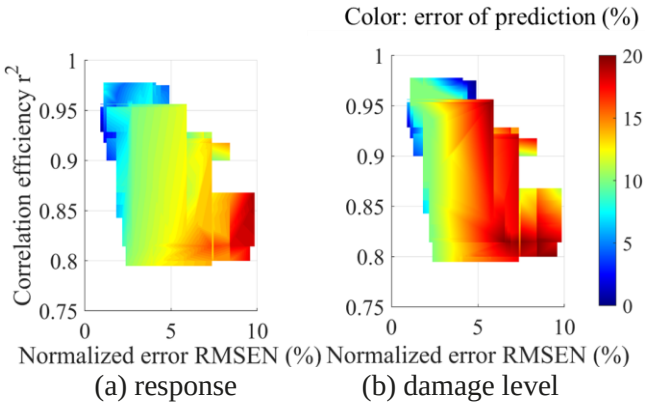

Figure 18: Updated damping & prediction

The relationship between the updated damping curve and the error of prediction is plotted in Fig. 18. For increases of r^2 and decreases of $RMSE_N$, the error in prediction tends to decrease.

Compared with the results of the performance curve, the relationship between error and damping is more clear and this indicates that the error in future response prediction is influenced more by the updated damping curve. For the cases investigated in this paper, if r^2 exceeds 0.9 and $RMSE_N$ is smaller than 5%, the error of prediction is no larger than 10% as suggested by the blue region in Fig. 19.

6 CONCLUSION

In this paper, the influence of differences between analytical model and observed behavior on prediction of future response is studied. An updating method is applied to performance and damping curves to match observations. The following three conclusions are drawn:

- After updating the performance and damping curves, more than 80% of the studied cases result in a more accurate prediction, and the average error in response decreases from approximately 20% to 10%.
- As the intensity of the earthquake producing the future response increases, and the ductility factor of the considered run increases from 3 to 5, over 90% of the studied cases tend to have larger errors. But the average error is not larger than 15% for response prediction, which is reasonable for practical use of the method.
- The updated performance curve has less influence on the prediction of response and damage level compared with the updated damping curve.

7 ACKNOWLEDGEMENT

This work was supported by JAEA Nuclear Energy S&T and Human Resource Development Project (Grant Number JPJA21P12345678, Principal researcher: Prof. Masaki MAEDA, Tohoku University) and JSPS KAKENHI Grant-in-Aid for Fostering Joint International Research (B), Grant Number JP21KK0074.

8 REFERENCE

Building Center of Japan (BCJ) (2016). "*The Building Standard Law of Japan*", edited by Building Center of Japan, Building Center of Japan, Tokyo, Japan. (in Japanese)

Datta T (2010), "*Seismic analysis of structures*". John Wiley & Sons, Ltd., New York, The United States, pp. 369. DOI:10.1002/9780470824634

Edo H and Takeda T (1977), "*Inelastic Earthquake Response of Reinforced Concrete Buildings*," Summaries of technical papers of 52nd annual meeting of Architectural Institute of Japan. (in Japanese)

Miura, K., Fujita, K., Tabata, Y., Maeda, M., Shegay, A. and Yonezawa, K. (2021). "*Shake-table test of a 4-storey frame-wall RC structure to investigate the collapse mechanism and safety limit*", Journal of Structural and Construction Engineering, 86(780): 247–257. (in Japanese) https://doi.org/10.3130/aijs.86.247

Takeda T, Sozen M A, and Nielsen M N (1970), "*Reinforced Concrete Response to Simulated Earthquakes*", Journal of the Structural Division, 96(ST12): 2557-2573. https://doi.org/10.1061/JSDEAG.0002765

Xu K, and Mita A (2021), "*Estimation of maximum drift of multi-degree-of-freedom shear structures with unknown parameters using only one accelerometer*", Structural Control and Health Monitoring, 28(e2799): 1-20. https://doi.org/10.1002/stc.2799

Yi Z, Oono A, Monical J and Maeda M (2023), *"Response Prediction and Damage Evaluation of a Reinforced Concrete Structure based on Limited Sensor Data and the Kalman Method"* Japan Concrete Institute (JCI) Annual Convention 2023, 45(2): 223-228. https://data.jci-net.or.jp/data_html/45/045-01-2035.html